JPL Document D-71127

TECHNOLOGY DEVELOPMENT FOR EXOPLANET MISSIONS (TDEM)

Assessing the performance limits of internal coronagraphs through end-to-end modeling

Technology Milestone #2 Whitepaper

John Krist, PI
Ruslan Belikov
Dimitri Mawet
Dwight Moody
Laurent Pueyo
Stuart Shaklan
John Trauger

7 December 2011

Approvals
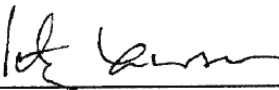
Released by

_____   15 Nov 2011
John E. Krist
Principal Investigator, JPL

Approved by
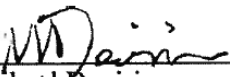
_____   11/15/2011
Peter R. Lawson,
Exoplanet Exploration Program Chief Technologist, JPL

_____   11/15/2011
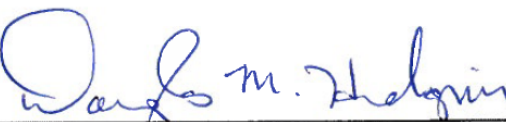Marie Levine,
Exoplanet Exploration Program Technology Manager, JPL

_____   11/15/2011
Michael Devirian,
Exoplanet Exploration Program Manager, JPL

_____   11/29/2011
Douglas Hudgins,
Exoplanet Exploration Program Scientist, NASA HQ

_____   28 Nov 2011
Lia LaPiana,
Exoplanet Exploration Program Executive, NASA HQ

Table of Contents

TDEM Milestone #2 White Paper: Assessing the Performance Limits of Internal Coronagraphs through End-to-End Modeling

1. Objective

In support of NASA's Exoplanet Exploration Program and the ROSES Technology Development for Exoplanet Missions (TDEM), this whitepaper explains the purpose of the TDEM Milestone #2 for our study, which is an assessment of the theoretical performance limits of selected coronagraphs as derived through numerical end-to-end modeling of a system with realistic optical aberrations. This milestone will use the propagation algorithms developed and verified in Milestone #1 (Krist et al. 2011) to characterize the wavefront control behavior of each coronagraph as predicted by numerical simulations (rather than hardware testing) and identify the limiting factors for achieving 10^{-10} contrast over a broad bandpass. This will help define the instrumental, testbed, and space mission configurations necessary to demonstrate and operate at this level using realistic technologies.

This whitepaper details only those aspects relevant to Milestone #2. The reader should review the Milestone #1 whitepaper (Krist et al. 2010) and SPIE Proceedings (Krist et al. 2011) for details on the context for the overall investigation, the coronagraphic technologies under study (hybrid bandlimited coronagraph (HBLC), vector vortex coronagraph (VVC), and phase-induced amplitude apodization (PIAA)), and the associated wavefront propagation algorithms.

2. Introduction

The technology milestone described here serves to gauge the developmental progress of optical modeling for a space-based coronagraphic mission such as ACCESS (Trauger et al. 2008) or the Terrestrial Planet Finder Coronagraph (TPF-C; Traub et al. 2006) that would detect and characterize exoplanets. Completion of this milestone is to be documented in a report by the Principal Investigator and reviewed by the Exoplanet Exploration Program and NASA HQ.

2.1. Coronagraphic wavefront control

Having the means to simulate propagation of a wavefront through a system, as developed in Milestone #1, is not sufficient to predict the contrast limit of a given telescope and coronagraph. Each coronagraph responds differently to wavefront aberrations and sets particular limits on the ability to control those errors with deformable mirrors, especially over a broad wavelength range (Shaklan & Green 2006). Therefore, the models must be executed within a wavefront control framework like that used in real systems that senses the simulated electric field at the image plane and then determines the deformable mirror

(DM) actuator settings necessary to minimize the scattered light around the star (Give'on et al. 2007; Krist, Trauger, & Moody 2006; Krist et al. 2009).

There are advantages to simulating the various coronagraphs using the same basic framework. The performance of each coronagraph can be compared to the others on even terms, given that the same front-end aberrations and wavefront control methods are used. Piecing together the results from different studies with varying layouts and modeling methods will not provide the consistency necessary to identify the true capabilities of each coronagraph. Unforeseen and perhaps subtle causes for the poor performance of a coronagraph might be more readily identified by comparing its behavior to the others, especially how each responds to changes in the wavefront caused by the deformable mirrors. Any problems can be diagnosed as being system-level (if all coronagraphs have poor performance) or particular to just one coronagraph (or its modeling technique).

Using simulations to determine how a coronagraph responds to wavefront control is critical to demonstrating the technological readiness of these systems. Prior to building and installing a coronagraph on a testbed, modeling can be used to decide what configuration may be required to provide the required performance (e.g., the location and surface quality of critical optics, the number and positioning of DMs, etc.). It can also highlight differences between testbed and proposed mission layouts. For example, PIAA testbed experiments so far (Belikov et al. 2009) have used a single DM *after* the PIAA optics (after the beam has been remapped and apodized), but some proposed mission concepts use two DMs located *before* PIAA, prior to wavefront remapping, to provide the maximum outer working angle. This study will be the first to accurately simulate the performance of PIAA in such a flight-like layout.

2.2. Goals of this study

Our study is specifically aimed at determining if there are fundamental, wavefront-modifying properties of the various coronagraph designs that, when used in a realistically aberrated system with wavefront control, would prevent attaining 10^{-10} contrast, the commonly accepted level for Earth-twin visible-light, imaging missions. A coronagraph only suppresses the diffraction pattern produced by the telescope. If the optical system is perfect and all the light is concentrated in the diffraction pattern, then any of the three designs used here (HBLC, VVC, PIAA) would be able to suppress the starlight to below 10^{-10} contrast, by design. However, any real system has aberrations that create speckles of scattered light that must be suppressed using wavefront control (deformable mirrors). A coronagraph, even one whose components are perfect, may alter the aberrations in a manner that prevents the wavefront control system from reducing the errors below the desired level. This may be due to wavefront remapping, conversion of phase errors to amplitude errors, etc. Such behavior may not be readily apparent until the coronagraph is implemented in an aberrated system with wavefront control. Due to the expense of hardware and testbeds, it is prudent to first predict the coronagraphic performance using end-to-end modeling in a simulated, realistically-aberrated system.

Using the propagation algorithms established in Milestone 1, we will conduct end-to-end numerical modeling of each coronagraph in a realistic optical system with wavefront

control to determine its contrast performance limits over a λ = 500 – 600 nm bandpass. The mean contrast will be predicted in an imaging field of dimension *r* = 2.5 – 18 λ_c/D (λ_c = 550 nm) around the central source. Wavefront control algorithm parameters will be determined, computational requirements identified, and the unique responses of each coronagraph to wavefront errors characterized.

The model system parameters will be modified as necessary (reduced surface errors, reordered layouts) to numerically simulate predicted performance that meets the required contrast. Changes beyond the current state of the art will be noted. As an example, preliminary modeling work for Milestone #2 for PIAA (Krist et al., 2011) shows that the measured, as-fabricated errors at the edge of currently best-available M1 optic are too large to provide the necessary contrast. By iteratively adjusting the surface errors at the edge of the measured map, we found that they need to be 20× lower, though this requirement may be beyond the current fabrication capabilities. This implies a sensitivity to fabrication errors, but not a fundamental design limitation. Due to the wavefront remapping action of PIAA, a 3rd DM would be needed after the forward PIAA optics to correct optical errors introduced while in remapped space. This is a design limitation.

We note that this study is purely concerned with numerical modeling of the coronagraphs. It does not involve any actual hardware implementations of the systems, such as testbeds like HCIT. The goal here is to understand the behavior of the coronagraphs before dedicating resources to placing them in testbeds or telescopes.

We intend to document everything we have learned in an appendix to the milestone results report (whose body would be concerned specifically on what milestone requirements were met).

2.3. Application to future NASA missions

Any future mission that uses one of these coronagraphs will require the algorithms and parameters derived in this study to

- Determine the performance of the coronagraph in real-world conditions
- Plan testbeds used to evaluate prototype and flight coronagraphs that properly replicate flight layouts and properties
- Define system layouts and optical parameters that provide sufficient performance
- Generate the DM response matrix that is used on-orbit for determining the DM settings that produce a dark hole in the image plane around the star that allows for high contrast imaging

2.4. Caveats

The modeling undertaken in this study assumes scalar propagation of the wavefront. Vector propagation, which includes the physical effects of electric field interactions with conductive and non-conductive materials at small scales, is not used. Vector propagation becomes important when small apertures may act as waveguides and the electrical

properties of the aperture substrate are significant (Lieber et al. 2005). In this study the impact of any vectorial effects would be mainly in the PIAA binary post-apodizer, the small occulting spot at the center of the VVC mask, and the amplitude-modifying structure of the HBLC. Based on previous studies for the Terrestrial Planet Finder Coronagraph, we expect such effects to be small as these structures are thin (i.e. we are not using thick apertures such as those used for early shaped pupil experiments). The realm of vector propagation is well beyond the time and financial limits of this study. We note that although the models do not use vector propagations, the HCIT laboratory results to date are consistent with predictions using scalar models to contrasts of 10^{-9} broadband and 2×10^{-10} narrowband.

We also do not account for the effects of polarization. It is known that polarization-induced aberrations can limit contrast at the levels we are concerned with here ($\sim 10^{-10}$) in all of the coronagraphs being considered (Elias et al. 2004; Balasubramanian et al. 2011). These can be minimized to some degree with judicious choices for coatings and system layouts, but they cannot be completely negated. We therefore assume that our simulations represent one polarization channel. It is known that the VVC requires a single polarization to provide broadband contrast at the 10^{-10} level.

This study also does not attempt to replicate a realistic on-orbit wavefront sensing and control sequence in which the telescope pointing and thermal effects in the optics cause wavefront changes over time. The goal here is to understand the fundamental limits of a static system with the understanding that it represents the best case scenario for a dynamic one.

This study does not include time-dependent wavefront variations due to stresses from the thermal and dynamic environment as might be experienced in flight. Whereas these factors are important for the relative comparison of coronagraph methods, they are beyond the scope of this study.

The only sources of contrast degradation that are modeled are those internal to the optical system diagramed in Figs. 1 and 2 of Section 7. Other sources of contrast loss, external to the instrument, would need to be considered as part of a more comprehensive error budget in future modeling studies.

3. Milestone #2 Description

Using the algorithms established in Milestone 1, we will assess the relative performance of HBLC, VVC, and PIAA coronagraphs via end-to-end modeling in a realistic optical system with wavefront control to achieve a numerically-predicted mean contrast of 10^{-10} within a specified annulus centered on the star integrated over a ~20% bandpass. Representative parameters of the optical system and wavefront control subsystem required to meet this contrast requirement will be derived.

3.1. Milestone Prerequisites

3.1.1 Contrast definition

Contrast, as it is used in this study, is defined as the ratio of the peak pixel value of an unocculted star image to the mean per-pixel surface brightness measured within a specified field around the star. A field contrast of 10^{-10} would indicate that a field point source (planet) 10^{10} times fainter than the star would have a peak pixel value equal to the mean per-pixel field brightness. The image fields in our study are sampled at 0.4 λ/D radians/pixel at $\lambda = 500$ nm (1.2× better than Nyquist).

3.1.2 Coronagraph contrast and image plane field dimensions

The imaging field of concern is an annulus centered on the star extending between $r = 2.5 \lambda_c/D - 18 \lambda_c/D$ radians in the image plane measured across a $\lambda = 500 - 600$ nm bandpass ($\lambda_c = 550$ nm, D = telescope diameter). The inner radius is set by the 50% transmission point of the occulter. The outer radius is set by the number of deformable mirror actuators across the pupil (46 in this study) and the shortest passband wavelength (18 $\lambda_c/D \approx 20 \lambda/D$ at $\lambda = 500$ nm). All of the coronagraphic designs evaluated in this study have been tailored to provide *in an aberration-free system* a mean contrast of $<10^{-10}$ within this field.

3.1.3 Optical system layout

The same optical system layouts used for the efficiency tests in Milestone #1 will be used for Milestone #2. There are two layouts; one common to VVC and HBLC and one for PIAA (see the Appendix). Both systems include two deformable mirrors in series for wavefront control. The systems are identical up to the 2nd DM. The system is represented as an unfolded (linear) layout and implemented using the PROPER optical propagation software (Krist 2007) with the custom routines developed in Milestone #1 specific for the coronagraphs.

3.1.4 Wavefront control

The wavefront will be controlled using two deformable mirrors with 46 actuators across the pupil. The DM is modeled by PROPER using measured actuator surface influence functions of the Xinetics DM used in the HCIT. In these simulations, the DM actuators piston exactly by the commanded amount, unlike those in real DMs which typically have

10% piston errors (these errors eventually iterate out and a precision of 0.3 Angstroms can be achieved). The wavefront control algorithm is Electric Field Conjugation (EFC; Give'on et al. 2007). Rather than using DM probing to sense the complex field at the final focus from intensity images, as is done in real systems, the computed field will be used directly.

3.2. Milestone Requirements

Milestone #2 Requirement: *Numerical models of each coronagraph will attempt to predict, after wavefront correction with deformable mirrors, a contrast of $\leq 10^{-10}$ in a realistically-aberrated optical system, quantified as the predicted mean level within a 2.5 – 18 λ_o/D annulus centered on the star over a $\lambda = 500 – 600$ nm bandpass. For all three coronagraphs, the optical system will be the same, including all simulated surface errors, from the primary mirror up to the second deformable mirror.*

Rationale:

Contrast

The brightness contrast relative to the star of an Earth-twin is $\sim 10^{-10}$ at visible wavelengths. The signal from the planet must be distinguished from the instrumentally-produced speckles inside the dark hole field around the star. We assume that this can be adequately accomplished in noisy images using post-processing (e.g. roll subtraction or reference star subtraction) if the peak pixel of the planet's point spread function is equal to the mean per-pixel speckle brightness.

Bandpass

In a real system, the contrast must be achievable over a broad ($\sim 20\%$) bandpass to either allow for deep integration in a wide bandpass filter or measurement using a spectrograph.

Field annulus

The inner radius is set where the occulter transmission is 50%. The outer radius is limited by the number of actuators on the DM.

Aberrations

To maximize the validity of comparisons among the coronagraph types, the optical systems need to be as identical as possible with the same fabrication errors. The HBLC and vector vortex coronagraphs can utilize the same optical system, excluding differences in the focal plane and Lyot masks. The PIAA coronagraph requires a different optical system after the second deformable mirror. Therefore, the optical system will be the same up to and including DM #2.

Each surface will have realistic phase errors (from figuring and polishing) and amplitude errors (from coating non-uniformities). Synthetic two-dimensional error maps will be generated from power spectral density curves derived from actual optics, and they will have achievable error levels. The primary mirror will have an RMS wavefront ($2\times$ surface) error of 8 nm, the secondary mirror 2.7 nm, and other optics >1.0 nm (the current

6

manufacturing limit for D ≈ 20 cm optics is ~0.13 nm RMS for EUV lithography). Interferometrically-measured surface error maps of the current best set of PIAA optics will be used for those surfaces, as they have aberration patterns unique to PIAA. They will be modified as necessary to provide the required contrast.

3.3. Milestone Metrics

Milestone #2 Metric:

The mean contrast will be predicted within the specified annular region integrated over a $\lambda = 500 - 600$ nm passband.

Rationale:

The simulation of the aberrated system will begin with the DMs set flat. The entering wavefront will be propagated through the system to the final focus where the complex-valued field will be measured (sensed) within the specified annulus around the star. This is done separately at five monochromatic wavelengths that evenly span the broad passband. The measured fields, along with the DM response matrix (see Milestone #1), will be used by EFC to determine DM actuator settings that will reduce the light within the annulus. The sense-control-propagate process repeats until convergence occurs (usually within 10 iterations from previous experience with simulations, given the perfect functionality of the DMs).

 Contrast at the end of each iteration will be measured by:

- Converting each of the five monochromatic fields (E_λ) to intensity: I = sqrt(abs[E_λ])

- Adding the monochromatic images together to create a broadband image

- Dividing the broadband image by the peak pixel value of the unocculted stellar PSF (accounting for the occulter radial transmission profile) to convert it to units of contrast

- Computing the mean of the pixels within the annulus

If, after convergence, the mean contrast is >10^{-10}, adjustments will be made to the system layout, optical errors, and/or EFC settings (e.g., regularization), and the process will be repeated. The elements and physical effects causing the control limitations will be identified.

4. Success Criteria

The following items summarize the requirements and metrics detailed in Sections 2 and 3.

4.1 The optical systems being modeled will include the elements required to implement realistic coronagraphs and a telescope, including two deformable mirrors in series for wavefront control (46 actuators across the beam). These systems will be identical up to and including the second deformable mirror.

4.2 The optics will have realistic surface (phase) and coating (amplitude) errors derived from actual optics.

4.3 The wavefronts will be propagated from surface to surface using the PROPER library for IDL along with the coronagraphic propagation and representation codes developed and verified in Milestone #1.

4.4 The fields of interest at the final focus will each be an annulus of $2.5\ \lambda_c/D \leq r \leq 18.0\ \lambda_c/D$ radians centered on the star ($\lambda_c = 550$ nm, D = diameter of the primary).

4.5 The wavelength bandpass will be $\lambda = 500 - 600$ nm. It will be evenly sampled at 5 monochromatic wavelengths to both sense the field and produce the polychromatic image.

4.6 Electric Field Conjugation will be used to determine deformable mirror settings that produce a high-contrast field in each coronagraphic system integrated over a $\lambda = 500 - 600$ nm bandpass (uniform weighting across λ).

4.7 The mean contrast within each dark hole field will be reported, where contrast is the per-pixel intensity divided by the peak of the unocculted stellar point spread function.

4.8 The optical system parameters will be iteratively modified to show simulated system performance that achieves 10^{-10} or better contrast within the dark hole. See the appendices in the Milestone #1 whitepaper for descriptions of the layouts, coronagraphs, and propagators.

5. Milestone Certification Data Package

The results of this study will be reported to and reviewed by the Exoplanet Exploration Program and NASA Headquarters. The documentation and data products which provide evidence that the requirements of this milestone have been met will be:

a. Documentation detailing the modeled optical system layouts, optical surface characteristics, and wavefront control algorithm parameters. This includes the PROPER optical prescriptions (text files) and the error maps for each optic (FITS files). The unique wavefront control behaviors of each coronagraph will be discussed. Recommendations for future work, testbed and flight configurations, and computer resources (for wavefront control) will be provided.

b. The fields at the final image planes, in units of contrast, which demonstrate that the milestone contrast requirement has been met. These will be distributed as FITS files and shown as color-coded contrast maps in the documentation.

c. Contrast maps at each required contrast level for each coronagraph as generated by the efficient algorithms. These will be distributed as FITS files and as color-coded maps in the documentation.

6. References

Belikov, R., Pluzhnik, E., Connelley, M. S., Lynch, D. H., Witteborn, F. C., Cahoy, K., L., Guyon, O., Greene, T. P., McKelvey, M. E., "First results on a new PIAA coronagraph testbed at NASA Ames," *Proc SPIE* 7440, 74400J (2009).

Give'on, A., Kern, B., Shaklan, S., Moody, D., Pueyo, L., "Broadband wavefront correction for high-contrast imaging systems," *Proc. SPIE,* 6691, 66910A (2007).

Krist, J., Belikov, R., Mawet, D., Moody, D., Pueyo, L., Shaklan, S., Trauger, J., "Assessing the performance limits of internal coronagraphs through end-to-end modeling: Technology Milestone #1 Whitepaper", JPL Document D-66100 (2010).

Krist, J., Moody, D., Mawet, D., Trauger, J., Belikov, R., Shaklan, S., Guyon, O., Vanderbei, R., "End-to-end simulations of different coronagraphic techniques," *Proc. SPIE*, 7440 (2009).

Krist, J., Belikov, R., Pueyo, L., Mawet, D., Moody, D., Trauger, J., Shaklan, S., "Assessing the performance limits of internal coronagraphs through end-to-end modeling: a NASA TDEM study," *Proc. SPIE*, 8151 (2011).

Krist, J., "PROPER: An optical modeling program for IDL," *Proc. SPIE*, 6675, 66750P (2007).

Krist, J., Trauger, J., Moody, D., "Studying a simple TPF-C", *Proc. SPIE*, 6265 (2006).

Lieber, M., Neureuther, A., Ceperley, D., Kasdin, J., Hoppe, D., Eisenman, A., "Evaluating the end-to-end performance of TPF-C with vector propagation models: Part I – pupil mask effects," *Proc. SPIE*, 5905, 59050K (2005).

Shaklan, S., Green, J., "Reflectivity and optical surface height requirements in a broadband coronagraph. 1.Contrast floor due to controllable spatial frequencies," *Applied Optics*, 45, 5143 (2006).

Traub, W., et al., "TPF-C: status and recent progress," *Proc. SPIE*, 6268, 62680T (2006).

Trauger, J., Stapelfeldt, K., Traub, W., Henry, C., Krist, J., et al. "ACCESS: a NASA mission concept study of an actively corrected coronagraph for exoplanet system studies," *Proc. SPIE*, 7010, 701029 (2008).

7. Appendix

The schematic layouts of the two coronagraphic systems are shown here.

Collimating OAP 1

Fold 1

DM 2

DM 1

Occulter/Vortex

Fold 2
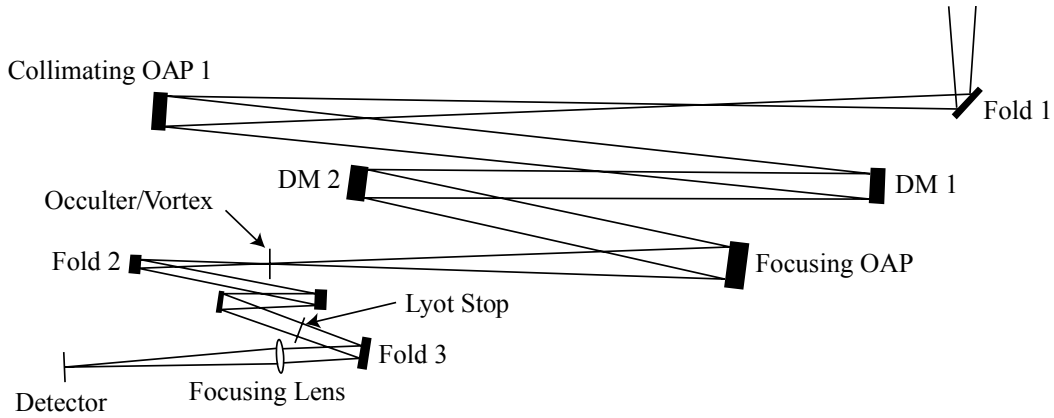
Focusing OAP

Lyot Stop

Fold 3

Detector

Focusing Lens

Figure 1. Schematic optical layout for the HBLC/VVC. Not shown are the telescope primary and secondary mirrors that feed Fold 1 in the upper right.

Collimating OAP 1

Fold 1

DM 2

DM 1

PIAA OAP 1

Fold 2

PIAA OAP 2

PIAA M1

PIAA M2

Collimating OAP 2

Post-Apodizer Mask

Focusing OAP

Reverse PIAA M1

Occulting Mask
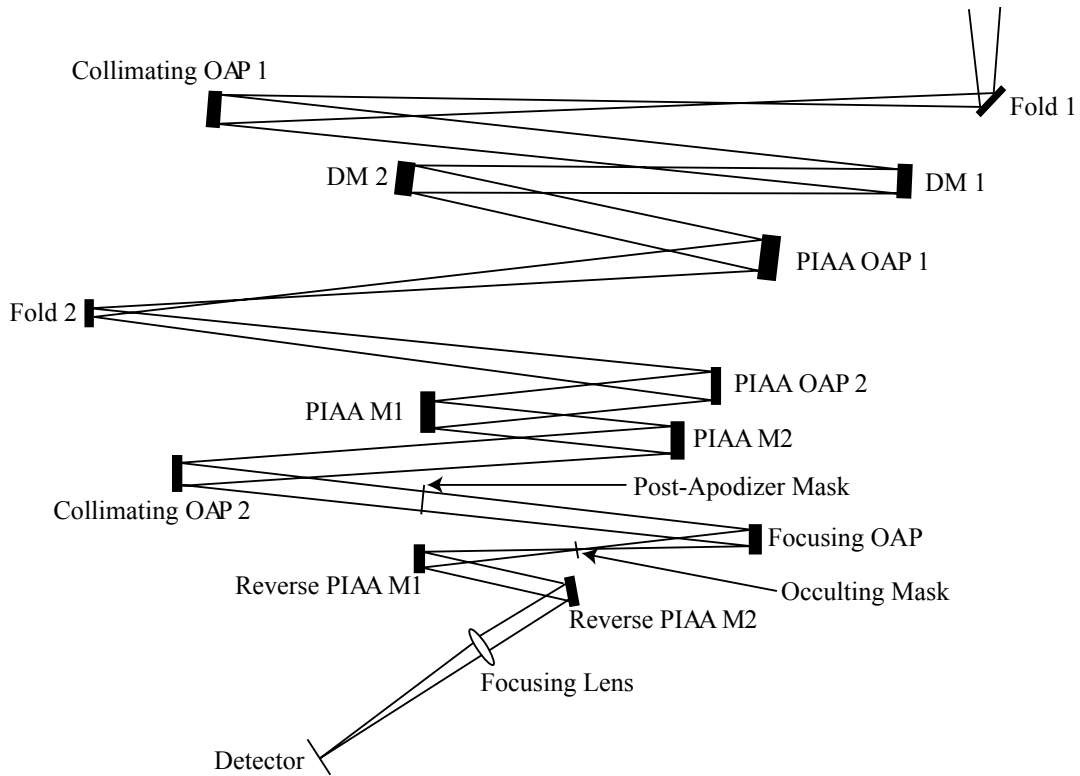
Reverse PIAA M2

Focusing Lens

Detector

Figure 2. Schematic optical layout for the PIAA coronagraph. Not shown are the telescope primary and secondary mirrors that feed Fold 1 in the upper right.